International Conference on Applied Energy 2019
Aug 12-15, 2019, Västerås, Sweden
Paper ID: 1010

FORMATION AND DISSOCIATION OF LAYERED HYDRATE IN SEA MUDS

Zhang Yu[1, 2, 3, 4], Li Xiaosen[1, 2, 3, 4,*], Wang Yi[1, 2, 3, 4], Chen Zhaoyang[1, 2, 3, 4], Li Gang[1, 2, 3, 4]

[1] Guangzhou Institute of Energy Conversion, Chinese Academy of Sciences, Guangzhou 510640, P. R. China

[2] Key Laboratory of Gas Hydrate, Chinese Academy of Sciences, Guangzhou 510640, P. R China

[3] Guangdong Provincial Key Laboratory of New and Renewable Energy Research and Development, Guangzhou 510640, P. R China

[4] Guangzhou Center for Gas Hydrate Research, Chinese Academy of Sciences, Guangzhou 510640, P. R China

ABSTRACT

Natural gas hydrate has currently been recognized as a potential alternative to traditional energy resources. In this study, the layered hydrate, which is a kind of grain-displacing hydrate, was synthetized in sea muds from South China Sea, and its dissociation behaviors by depressurization with different ambient temperature were investigated. The experimental results indicated that the cumulative gas production increases quickly with the pressure decrease. When the pressure reaches the setting production pressure and keeps constant, the gas production rate decreases significantly. The hydrate dissociation rate increases with the increase of the ambient temperature. There are obvious layered hollows in sea muds after hydrate dissociation. The sediment deformation cannot be ignored during the gas recovery from layered hydrate in sea muds.

Keywords: Hydrate, layered, sea muds, dissociation, depressurization

Corresponding author. Tel: +86 20 87057037. Fax: +86 20 87057037.
E-mail address: lixs@ms.giec.ac.cn.

1. INTRODUCTION

With increasing energy demands and the continued consumption of conventional oil and gas resources, the supply of and demand for oil and gas have become increasingly prominent. Since natural gas hydrate is the attributes of high energy density and large reserves, it is currently recognized as a potential strategic energy resource for finite resources [1–3].

There are different types of concentrated gas hydrate, such as seafloor hydrate mounds, grain-displacing hydrate and pore-filling hydrate in sands [4, 5]. Boswell and Collett [6] evaluated the potential technical recoverability of different type gas hydrate. Grain-displacing hydrate is considered to have a potential recoverability. However, there have been no field tests or published numerical modeling studies on the production feasibility of grain-displacing hydrate.

Recently, the hydrate dissociation behaviors via the depressurization method have been investigated through a variety of experimental and numerical studies [7-9]. Due to the different properties of the different types of concentrated gas hydrate, the dissociation behaviors for different types of concentrated gas hydrate should be different, including the gas production behaviors, the hydrate dissociation evolution, and the changes of the reservoir structure. However, the experimental investigations on these problems were not reported in the literatures.

In this work, a cubic reactor was applied to investigate methane hydrate formation and dissociation in sea muds under the geological conditions of the hydrate reservoir in the South China Sea. The layered hydrate, which is a kind of grain-displacing hydrate, was synthetized in sea muds from South China Sea, and its dissociation behaviors by depressurization were investigated.

2. EXPERIMENTAL SECTION

2.1 *Materials*

The methane with the purity of 99.9% was obtained from Fushan Hua Te Gas Co. The sea mud supplied by Guangzhou Geological Survey was from the Shenhu Area in the South China Sea. The physical properties of the sea muds are listed in Table 1.

Selection and peer-review under responsibility of the scientific committee of the 11th Int. Conf. on Applied Energy (ICAE2019).

Table 1 The detail properties of sea mud

Property	Value
Density g/ml	2.81
Average particle diameter μm	7.898
Specific area m^2/g	16.412
Average pore diameter nm	12.178
Pore volume ml/g	0.04997

2.2 Apparatus

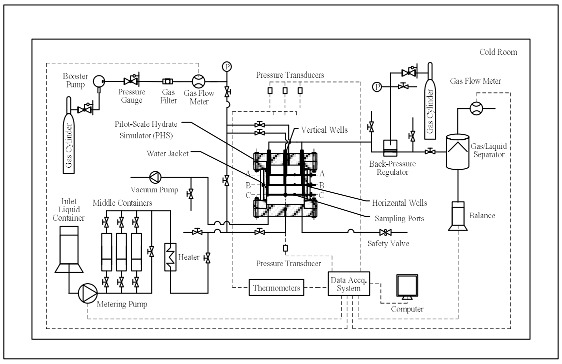

Fig. 1 Schematic diagram of the experimental apparatus.

Fig. 1 shows the experimental apparatus schematic. Fig. 2 shows the temperature measurement points and wellheads distribution. As seen in Fig. 1a, the experimental apparatus consists of a cubic high-pressure reactor, a temperature-controlling water bath, a back-pressure regulator, a gas-liquid separation system, a data acquisition system, and some measurement units. The cubic high-pressure reactor, which has 729 ml inner volume and is immersed in a temperature-controlled water bath, can withstand pressure up to 30 MPa. A vertical production well was placed in the middle of the reactor. As seen in Fig. 2, 27 Pt100 thermocouples were evenly distributed inside the reactor on three layers, specifically the top (A), middle (B), and bottom (C). Each layer was placed on 9 thermocouples that were measured at a temperature range of 223.15 K to 473.15 K and a currency of ± 0.1 K. Two pressure transducers (TRAFAG NAT 8251) were located at the inlet and the outlet, and measured at the range of 0 – 25 MPa and a currency of ± 0.02 MPa. The outlet flow reached the gas-liquid separator and was separated to gas and water, wherein the liquid flowed down to the container through an electronic scale (Santorius Co.) with the concrete vision Santorius BS 2202S (0–2200 g, ± 0.01 g) and the gas flowed to the flowmeter (Seven Star Co.) with vision D07-11CM (0–10 L/min, ± 2%). During the experimental procedure, the temperature, pressure, and volume of the cumulative gas production, are recorded by the data collection unit in time.

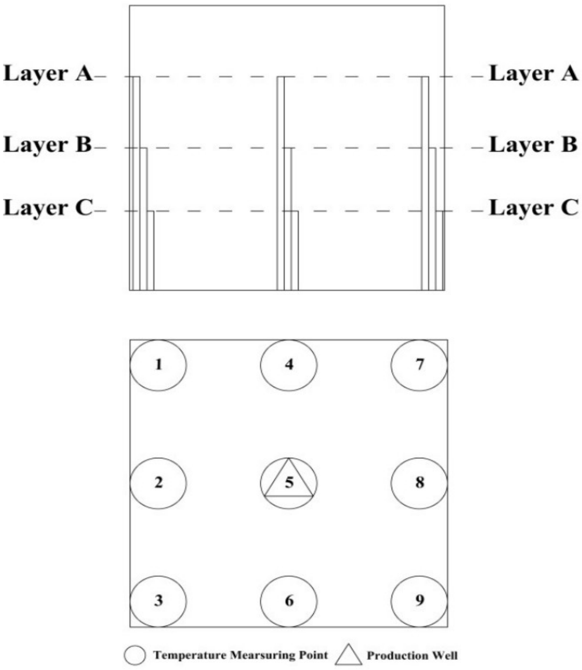

Fig. 2 Temperature Measurement Points and Wellhead Distribution Diagram.

2.3 Procedure

Fig. 3 Packed process of sea muds and ice particles.

Sea muds were dried at 373.15K for 24h and subsequently weighed to determine the dry samples at the room temperature. The reactor was firstly filled with sea muds with a height of 1cm, then filled with 30g ice powder. Subsequently, the sea muds and ice powder were packed into the reactor alternately until the reactor was full. The final amount of sea muds and ice powder filled into the reactor is 339g and 123g, respectively. The temperature of the water bath was set below 265.15 K. Afterwards, methane gas was injected into the reactor to pressurize the reactor up to 20 MPa. The ice particles directly turned into hydrate. Thus, the ice distribution turned into hydrate distribution. Therefore, the grain-displacing hydrate (layered) was synthesized.

After the hydrate formation, the hydrate dissociation experiments were carried out using depressurization. The temperature of the water bath was set to the experimental temperature and the production pressure was set to 4.70 MPa by the back-pressure regulator. Subsequently, the hydrate gradually decomposed and methane gas released from outlet. After hydrate was completely dissociated, residual methane gas in the reactor was released gradually, and the system pressure declined to atmosphere. During the hydrate dissociation, the data were recorded in real time. Finally, the top cover is opened to observe inner structure of the sea muds.

3. RESULTS AND DISCUSSION

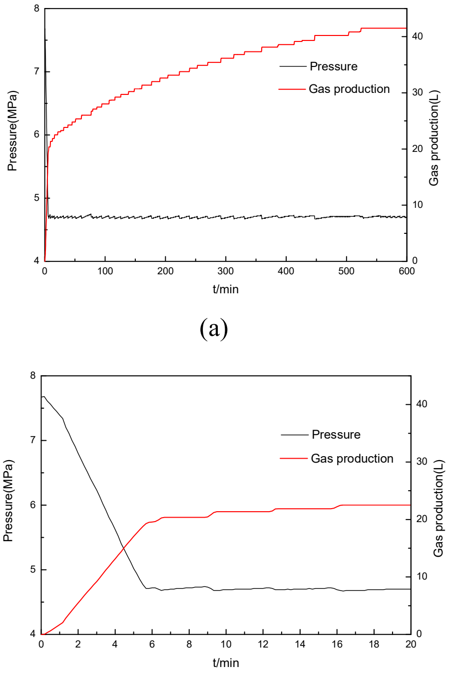

(a)

(b)

Fig. 4 Pressure and cumulative gas production changes during hydrate dissociation for experimental run 1.

In this work, two experimental runs were carried out to investigate the dissociation behaviors of layered hydrate in sea muds by depressurization. The experiments were performed at the ambient temperature of 7.0 ℃ (run 1) and 8.5 ℃ (run 2), respectively.

Fig. 4a gives the cumulative gas production and pressure changes during hydrate dissociation of experimental run 1. Fig. 4b gives the details of the first 20 min in Fig. 4a. From Figures 4a and 4b, it can be found that the cumulative gas production increases quickly with the pressure decrease. When the pressure reaches the setting production pressure and keeps constant, the gas production rate decreases significantly. During the depressurization period, the produced gas is mainly free gas in the reactor. In the steady-pressure period, the produced gas is dissociated from hydrate.

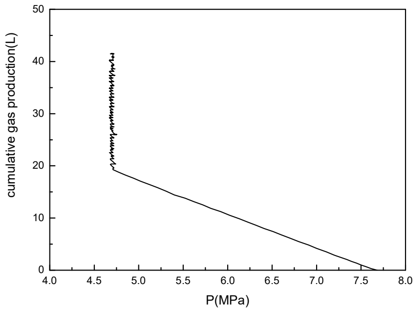

Fig. 5 Pressure and cumulative gas production changes during hydrate dissociation for experimental run 1.

Fig. 5 gives the changes of gas production with pressure in the reactor. As shown in Figure 6, the gas production has a good proportional relationship with the pressure in the reactor. It indicates that the hydrate dissociates little during the depressurization period, and the hydrate mainly dissociates in the steady-pressure period. It should be due to the fact that the depressurization duration is very short.

Fig. 6 gives the changes of hydrate dissociation ratio during hydrate dissociation of experiments 1 and 2. During hydrate dissociation, the hydrate dissociation ratio can be calculated as:

$$\varphi = \frac{N_d}{N_{ht}} \qquad （1）$$

Where N_d is the amount of the dissociated hydrate, N_{ht} is the initial hydrate amount before hydrate dissociation. From Fig. 6, it can be found that the hydrate dissociation rate decreases gradually, and the hydrate dissociation rate of experiment 1 is much lower than that of experimental run 2. In this study, the hydrate dissociation duration for experimental run 1 and run 2 is 524 min and 381 min, respectively. It indicates that the hydrate reservoir temperature has a significant effect on hydrate dissociation by depressurization. It has been found that hydrate dissociation is an endothermic process, and the heat needed for hydrate dissociation by depressurization should be transferred from the ambient in the hydrate should dissociate in the later stage. Therefore, for a higher ambient temperature, the heat transfer rate from ambient to hydrate reservoir is higher, resulting in a higher hydrate dissociation rate.

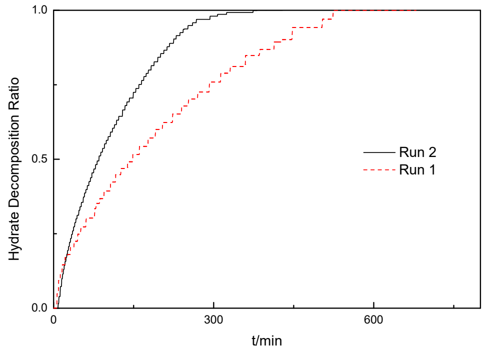

Fig. 6 Comparison of changes hydrate dissociation ratio during hydrate dissociation for experimental run 1 and run 2.

Fig. 7 Inner structure of sea muds after hydrate dissociation for Run2.

In Fig. 7, there are obvious layered hollows in sea muds after hydrate dissociation. The sediment deformation cannot be ignored during the gas recovery from layered hydrate in sea muds. The collapse of sea muds may happen after the hydrate dissociation due to the fact that the solid hydrate participates in constituting the structure of the hydrate reservoir. When the solid hydrate changes to liquid, the mechanical stability of the reservoir is destroyed [10].

4. CONCLUSIONS

In this work, methane hydrate dissociation in sea muds with layered hydrate accumulations is firstly investigated by experiments, and the influence of ambient temperature on the hydrate dissociation is analyzed. Experimental results indicate that the cumulative gas production increases quickly with the pressure decrease. When the pressure reaches the setting production pressure and keeps constant, the gas production rate decreases significantly. The hydrate reservoir temperature has a significant effect on hydrate dissociation by depressurization. The hydrate dissociation rate increases with the increases of the ambient temperature. There are obvious layered hollows in sea muds after hydrate dissociation. The sediment deformation cannot be ignored during the gas recovery from layered hydrate in sea muds.

ACKNOWLEDGEMENT

We are grateful for the support of the Key Program of the National Natural Science Foundation of China (No. 51736009), the National Natural Science Foundation of China (No. 51476174, 51576202, and 51676196), Special project for marine economy development of Guangdong Province (GDME-2018D002), and the National Key Research and Development Plan of China (No. 2016YFC0304002 and 2017YFC0307306).

REFERENCE

[1] Boswell R, Collett TS, Frye M, Shedd W, Mcconnell DR, Shelander D. Subsurface gas hydrates in the northern Gulf of Mexico. Mar Petrol Geol 2012;34:4-30.
[2] Chong ZR, Yang SHB, Babu P, Linga P, Li XS. Review of natural gas hydrates as an energy resource: Prospects and challenges. Appl Energy 2016;162:1633-52.
[3] Li XS, Xu CG, Zhang Y, Ruan XK, Li G, Wang Y. Investigation into gas production from natural gas hydrate: a review. Appl Energy 2016;172:286–322.
[4] Pooladi-Darvish M. Gas production from hydrate reservoirs and its modeling. J Petrol Technol 2004;56:65-71.
[5] Boswell R, Shipp C, Reichel T, Shelander D, Saeki T, Frye M, et al. Prospecting for marine gas hydrate resources. Interpretation-J Sub 2016;4:Sa13–24.
[6] Boswell R, Collett TS. Current perspectives on gas hydrate resources. Energy Environ Sci 2011;4:1206–15.
[7] Zhang Y, Li XS, Chen ZY, Wang Y, Ruan XK. Effects of hydrate saturation on the methane hydrate dissociation by depressurizaiton in sediments in a cubic hydrate simulator. Ind Eng Chem Res. 2015;54:2627-37.
[8] Wang Y, Li XS, Xu WY, Li QP, Zhang Y, Li G, et al. Experimental investigation into factors influencing methane hydrate formation and a novel method for hydrate formation in porous media. Energy Fuel 2013;27:3751–7.
[9] Haligva C, Linga P, Ripmeester JA, Englezos P. Recovery of methane from a variable-volume bed of silica sand/hydrate by depressurization. Energy Fuel 2010;24:2947–55.
[10] Zhang XH, Lu XB, Shi YH, Xia Z, Liu WT. Centrifuge experimental study on instability of seabed stratum caused by gas hydrate dissociation. Ocean Eng 2015;105:1–9.